*Anal. Chem.* **2006,** *78,* 2272−2278

# Quantitative 3D Mapping of Fluidic Temperatures within Microchannel Networks Using Fluorescence Lifetime Imaging

**Richard K. P. Benninger,† Yasemin Koç,‡ Oliver Hofmann,‡ Jose Requejo-Isidro,† Mark A. A. Neil,† Paul M. W. French,*,† and Andrew J. deMello*,‡**

*Department of Physics and Department of Chemistry, Imperial College London, Exhibition Road, South Kensington, London, SW7 2AZ, United Kingdom*



**We describe a novel method for quantitatively mapping fluidic temperature with high spatial resolution within microchannels using fluorescence lifetime imaging in an optically sectioning microscope. Unlike intensity-based measurements, this approach is independent of experimental parameters, such as dye concentration and excitation/detection efficiency, thereby facilitating quantitative temperature mapping. Micrometer spatial resolution of 3D temperature distributions is readily achieved with an optical sectioning approach based on two-photon excitation. We demonstrate this technique for mapping of temperature variations across a microfluidic chip under different heating profiles and for mapping of the 3D temperature distribution across a single microchannel under applied flow conditions. This technique allows optimization of the chip design for miniaturized processes, such as on-chip PCR, for which precise temperature control is important.**

Microfluidic chip-based systems have engendered many new opportunities in the physical and biological sciences. Such systems have been successfully applied to a number of fields, including cell manipulations and sorting,[1] molecular synthesis,[2] DNA analysis,[3] proteomics,[4] process control, immunoassays[5,6] and environmental monitoring.[7,8] The advantages associated with the downsizing or miniaturization of analytical systems are numerous and include improved efficiency with respect to sample size, control, response times, cost, analytical performance, component integration, throughput, and automation. For many applications, the ability to precisely measure and control sample temperature within microchannel environments is a prerequisite for efficient analysis or processing. For instance, in capillary electrophoresis, high applied electric field strengths often generate excessive Joule heat, which may not be efficiently dissipated. This phenomenon directly affects zone broadening and can lead to a reduction in separation efficiencies.[9] Similarly, a diversity of microfabricated devices for performing DNA amplification via PCR have been reported over the past decade.[10] Although their structure and operation have ranged widely, the gains afforded through miniaturization have been significant. The heart of these performance gains lies in improved thermal transfer on a small scale: heat can be inserted into and removed from microfluidic environments exceptionally quickly due to the high surface-to-volume ratios typical in such systems, and in principle, temperatures can be controlled throughout the sample volume. When performing PCR, the ability to accurately control system temperatures is especially important, since both primer annealing to single-stranded DNA and the catalytic extension of this primer to form the complementary strand will only proceed in an efficient manner within relatively narrow temperature ranges.[11] It is, therefore, imperative to be able to accurately monitor the temperature distributions in such microfluidic channels.

Accurate and spatially resolved temperature measurements in microfluidic devices are typically achieved through the use of external or integrated thermocouples.[12] Externally mounted thermocouples are unable to accurately monitor temperature variations within the fluidic system and only provide an estimate of the temperature of exterior chip surfaces. Furthermore, the thermocouples used in such measurements can themselves produce inordinately large heat losses while offering relatively low spatial resolution. Methods for integrating thermocouple contacts within microfluidic chip-based systems to allow direct measurement of fluidic temperatures that address some of these problems at the expense of increased fabrication complexity and limited

* To whom correspondence should be addressed. E-mails: a.demello@imperial.ac.uk, paul.french@imperial.ac.uk.
† Department of Physics.
‡ Department of Chemistry.

(1) Wang, M. M.; Tu, E.; Raymond, D. E.; Yang, J. M.; Zhang, H. C.; Hagen, N.; Dees, B.; Mercer, E. M.; Forster, A. H.; Kariv, I.; Marchand, P. J.; Butler, W. F. *Nat. Biotechnol.* **2005**, *23*, 83−87.
(2) Tian, J.; Gong, H.; Sheng, N.; Zhou, X.; Gulari, E.; Gao, X.; Church, G. *Nature* **2004**, *432*, 1050−1054.
(3) Service, R. F. *Science* **1998**, *282*, 396−399.
(4) Culbertson, C. T.; Jacobson, S. C.; Ramsey, J. M. *Anal. Chem.* **2000**, *72*, 5814−5819.
(5) Guijt, R. M.; Baltussen, E.; van Dedem, G. W. K. *Electrophoresis* **2002**, *23*, 823−835.
(6) Verpoorte, E. *Electrophoresis* **2002**, *23*, 677−712.
(7) Loy, A.; Schulz, C.; Luecker, S.; Schoepfer-Wendels, A.; Stoecker, K.; Baranyi, C.; Lehner, A.; Wagner, M. *Appl. Environ. Microbiol.* **2005**, *71*, 1373−1386.
(8) Brown, K. *Science* **2004**, *305*, 1228−1229.
(9) Petersen, N. J.; Nikolajsen, R. P. H.; Mogensen, K. B.; Kutter, J. P. *Electrophoresis* **2004**, *25*, 253−269.
(10) DeMello, A. J. *Nature* **2003**, *422*, 28−29.
(11) Yoon, D. S.; Lee, Y. S.; Lee, Y.; Cho, H. J.; Sung, S. W.; Oh, K. W.; Cha, J.; Lim, G. *J. Micromech. Microeng.* **2002**, *12*, 813−823.
(12) Nishikawa, T.; Kambara, H. *Electrophoresis* **1996**, *17*, 1115−1120.



10.1021/ac051990f CCC: $33.50 
Published on Web 03/04/2006

operational lifetimes have been reported.[13]

In recent years, a number of spectroscopic techniques have been applied to the measurement of temperature within microfluidic environments. Such approaches are advantageous because they are noninvasive, can directly measure fluidic temperatures, and potentially offer high spatial and temporal resolution (limited only by the imaging system employed). For example, Chaudhari et al. reported optical measurements of temperature uniformity in a microfabricated reactor array using encapsulated liquid crystals suspended in the contained liquid medium. Thermochromic liquid crystals (TLCs) exhibit a wavelength-dependent reflectivity that is strongly sensitive to temperature, within a range defined by their chemical composition, allowing local temperature quantification to within 0.1 °C through the hue.[14] One drawback, however, is that these crystals are comparatively large and can alter fluid flow characteristics. Nanoliter-volume proton nuclear magnetic resonance spectroscopy has also been used to monitor electrolyte temperature in capillary electrophoresis through measurement of the shift in the proton resonance frequency of water.[15] Intracapillary temperatures could be recorded noninvasively with subsecond temporal resolution without the addition of active probes to the fluid medium. Nevertheless, this technique suffers from limited spatial resolution due to the RF signal and probe size.[16] Morris and co-workers have utilized Raman spectroscopy to map both axial and radial temperature gradients in operating electrophoresis capillaries.[17] Intracapillary temperature variations could be measured through the temperature-sensitive OH stretching envelope of the water Raman spectrum, which is strong and free from spectral interferences. Such an approach affords a precision in temperature measurement of ±1 °C and a spatial resolution of 1−5 $\mu$m, but it is limited to single-point measurements, and acquisition times are high.[17,18] More recently, Easley et al. have reported the application of extrinsic Fabry−Perot interferometry using a broadband IR source for real-time temperature monitoring within microfluidic environments via the temperature-dependent refractive index of the fluid in the microchannel.[19] Finally, (steady-state) fluorescence-based spatial and temporal mapping of microfluidic temperature has been demonstrated by Ross et al.[20] This approach exploits the temperature dependence of the fluorescence quantum efficiency of many molecular dyes. In these reported studies, changes in the fluorescence intensity of a solution of rhodamine B were used to determine intrachannel temperature variations with a precision of ±3 °C, a spatial resolution of 1 $\mu$m, and a temporal resolution of 33 ms. Specifically, such measurements were used to estimate intrachannel temperature distributions resulting from Joule heating in electrokinetically pumped microfluidic systems. Although this method is elegant and relatively simple to implement, the primary problem when using steady-state fluorescence measurements is that the observed fluorescence intensity may be significantly affected by other experimental factors, such as spatial variation of excitation and detection efficiencies, concentration artifacts, pollution from scattered excitation light, reagent autofluorescence, and inner filter effects.

Ratiometric fluorescence techniques, including spectrally resolved, fluorescence lifetime-resolved, and polarization-resolved measurements, as well as fluorescence correlation spectroscopy, can address these issues by providing a readout signal that is independent of intensity (excitation and collection efficiency), fluorophore concentration, and photon path length. Fluorescence lifetime sensing is interesting for this application because the fluorescence lifetime, like the quantum efficiency, is a function of the radiative and nonradiative decay rate coefficients, which can be dependent on environmental parameters, such as temperature, viscosity, and pH. It is possible to select a fluorophore whose fluorescence lifetime varies predictably with temperature and, thus, use lifetime measurements to provide a quantitative (ratiometric) means of monitoring temperature distributions with no intensity artifacts.[21] Here, we demonstrate for the first time that fluorescence lifetime imaging (FLIM) can quantitatively image temperature distributions resolved in three spatial dimensions and can report the first application to directly quantify temperature within microchannel environments. Our approach, which includes the use of multiphoton excitation to achieve optical sectioning, allows for high spatial and temporal resolution, operates over a wide temperature range, and can be used to rapidly quantify local temperatures with high precision. We note that optical sectioning is important, not only to provide 3D data stacks but also to eliminate out-of-plane fluorescence that could contaminate the observed temperature distributions in the case of axial temperature gradients. This has not been explicitly considered in previous studies of temperature measurements within microfluidic systems. We note that FLIM has previously been applied to quantify other environmental properties, such as refractive index,[22] viscosity,[23] ion concentration,[24] and pH,[25] as well as nanoscale interactions using Förster resonant energy transfer (FRET).[26] To demonstrate the efficacy of FLIM applied to quantitative 3D mapping of fluidic temperatures, we present a description of the experimental setup, initial calibration studies, and its application within a simple microchannel network on a glass PCR microchip.

## EXPERIMENTAL SECTION

**Microfluidic System Fabrication.** Microfluidic devices were made in-house using direct-write laser lithography, wet chemical etching, and bonding techniques.[27] Briefly, a soda lime glass


(13) Burns, M. A.; Johnson, B. N.; Brahmasandra, S. N.; Handique, K.; Webster, J. R.; Krishnan, M.; Sammarco, T. S.; Man, P. M.; Jones, D. *Science* **1998**, *282*, 484−487.
(14) Chaudhari, A. M.; Woudenberg, T. M.; Albin, M.; Goodson, K. E. *J. Micromech. Syst.* **1998**, *7*, 345−355.
(15) Lacey, M. E.; Webb, A. G.; Sweedler, J. V. *Anal. Chem.* **2000**, *72*, 4991−4998.
(16) Lacey, M. E.; Webb, A. G.; Sweedler, J. V. *Anal. Chem.* **2002**, *74*, 4583−4587.
(17) Davis, K. L.; Liu, K.-L. K.; Lanan, M.; Morris, M. D. *Anal. Chem.* **1993**, *65*, 293−298.
(18) Liu, K.-L. K.; Davis, L.; Morris, M. D. *Anal. Chem.* **1994**, *66*, 3744−3750.
(19) Easley, C. J.; Legendre, L. A.; Roper, M. G.; Wavering, T. A.; Ferrance, J. P.; Landers, J. P. *Anal. Chem.* **2005**, *77*, 1038−1045.
(20) Ross, D.; Gaitan, M.; Locascio, L. E. *Anal. Chem.* **2001**, *73*, 4117−4123.
(21) Jeon, S.; Turner, J.; Granick, S. *J. Am. Chem. Soc.* **2003**, *125*, 9908−9909.
(22) Suhling, K.; Siegel, J.; Phillips, D.; French, P. M. W.; Lévêque-Fort, S.; Webb, S. E. D.; Davis, D. M. *Biophys. J.* **2002**, *83*, 3589−3595.
(23) Benninger, R. K. P.; Hofmann, O.; McGinty, J.; Requejo-Isidro, J.; Munro, I.; Neil, M. A. A.; deMello, A. J.; French, P. M. W. *Opt. Express* **2005**, *13*, 6275−6285.
(24) Agronskaia, A. V.; Tertoolen, L.; Gerritsen, H. C. *J. Biomed. Opt.* **2004**, *9*, 1230−1237.
(25) Sanders, R.; Draaijer, A.; Gerritsen, H. C.; Houpt, P. M.; Levine, Y. K. *Anal. Biochem.* **1995**, *34*, 302−308.
(26) Day, R. N.; Piston, D. W. *Nat. Biotechnol.* **1999**, *17*, 425−426.
(27) Effenhauser, C. S.; Manz, A.; Widmer, H. M. *Anal. Chem.* **1993**, *65*, 2637−2642.

substrate precoated with a positive photoresist (AZ 1518) and a low reflective chromium layer (Nanofilm, Westlake Village, California) was exposed using a DWL system (DWL2.0, Heidelberg Instruments, Heidelberg, Germany) to transfer the channel design. After the photoresist was developed (Microposit 351, Shipley Europe Ltd., Coventry, UK), channels were etched into the glass substrate using a buffered oxide etching solution ($HF-NH_4F$), and external access holes were drilled. The resulting microstructured channels in the glass substrate are 130 $\mu$m wide and ~38 $\mu$m deep. To form enclosed channels, a glass cover plate cleaned with concentrated $H_2SO_4$ was thermally bonded in a furnace (Heraeus Instruments GmbH, Hanau, Germany) at 585 °C. Fused-silica capillaries (375-$\mu$m o.d., 50-$\mu$m i.d.) were cemented to the inlet and outlet holes using a thermally cured two-part epoxy (Araldite 2014).

**FLIM Instrumentation.** Fluorescence is excited using 100-fs pulses at a repetition rate of 80 MHz from a mode-locked Ti:Sapphire laser (Mai-Tai, Spectra-Physics, Mountain View, CA), which is tunable between 700 and 1000 nm. With the laser tuned to 840 nm, the output beam is coupled to a quasi-wide-field, multibeam, multiphoton microscope (TriMScope, LaVisionBiotec GmbH, Bielefeld, Germany) that rapidly scans multiple parallel beams, generated using a cascaded beam-splitter system, over the whole field of view.[28] Multiphoton excitation[29] via a ×10 NA 0.25 air objective (Olympus) results in a femtoliter-sized excitation volume and, thus, provides inherent optical sectioning. The rapidly scanning array of excitation foci permits wide-field detection, allowing a greater fluorescence signal to be obtained per unit time as compared to conventional (single-beam scanning) multiphoton microscopes and, thus, faster image acquisition. FLIM is implemented using an ultrafast, electronically shuttered, wide-field detector based on a gated image intensifier. A more extensive description of this FLIM system is given elsewhere,[30,31] and a schematic of the essential elements is shown in Figure 1A. Briefly, fluorescence is imaged onto the photocathode of a time-gated intensifier (HRI, Kentech Instruments Ltd, Didcot, UK) and optically relayed to a CCD camera (Imager Intense, LaVision GmbH, Göttingen, Germany). The time-gated intensifier is synchronously switched from zero to high gain for periods of a few hundred picoseconds at adjustable delay times after excitation using a fast switching delay box (TDU, Kentech Instruments Ltd). A series of fluorescence intensity images, averaged over many excitation pulses, is acquired. These sample the fluorescence decay profiles (Figure 1B) for each pixel in the field of view, and the series of time-gated intensity values are fitted to an exponential decay model on a pixel-by-pixel basis, thereby producing a spatial map of fluorescence lifetime. For three-dimensional measurements, the imaging depth is adjusted between each full sampling of the fluorescence decay by moving the sample axially using an automatic focus stepper (MFD, Märzhäuser Wetzlar GmbH, Wetzlar-Steindorf Germany). Image acquisition is controlled by Imspector software (LaVisionBiotec, Bielefeld, Germany), and

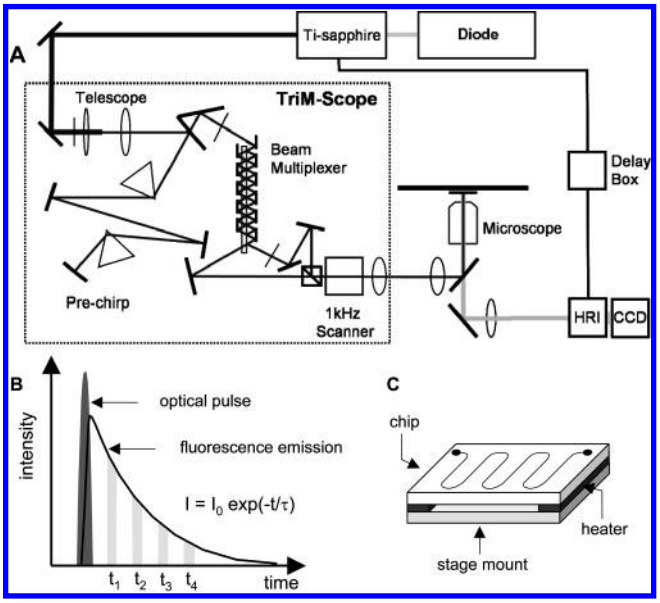


**Figure 1.** Schematic of 3D FLIM system for imaging microchannel temperature. (A) The 3D FLIM system. Pulsed infrared illumination is coupled into the TriMScope for beam multiplexing and scanning. This illumination is focused onto the sample, where two-photon absorption occurs in a thin optical section only. The fluorescence emission is then imaged onto a gated optical intensifier relayed to a CCD camera. Solid black lines indicate triggering connections. (B) Illustration of how the fluorescence decay is sampled by the gated optical intensifier. Images are acquired at varying time points, $t_n$, on the fluorescence decay and fitted for the fluorescence lifetime on a pixel-by-pixel basis. (C) The microfluidic chip mounted on the microchannel heater using heat-conductive paste. Rhodamine B is flowed through the microfluidic chip, while excitation and detection of fluorescence is carried out from below.

CCD scanning and delay switching are synchronized using a trigger pulse generator (DG535, Stanford Research Systems, Sunnyvale, CA).

**Microfluidic System Operation and Data Acquisition.** A syringe pump (Pump 11, Harvard Apparatus, Cambridge, MA) is used to deliver solutions of rhodamine B in methanol ($10^{-4}$ M) into the microfluidic system at volumetric flow rates between 0.1 and 10 $\mu$L/min from a 500-$\mu$L gastight syringe. Heating of the glass chip is performed by resting the substrate on two 5-W heating cartridges, with external surface temperatures being monitored using a Pt100 thin-film resistor mounted on the surface of the chip. Temperature controllers incorporate standard PID (proportional, integral, and derivative) digital temperature controllers (CAL 3200, CAL Controls Ltd, Hitchin, UK), power supplies, and switching electronics for the heating cartridges. A schematic of this arrangement can be seen in Figure 1C. Using this system, fluorescence lifetime imaging of fluid contained within the microchannel can be performed. Initially, a series of 20 time-gated intensity images is acquired, which are then fitted on a pixel-by-pixel basis to a single-exponential decay model with an offset that is included to account for background light and the digital CCD offset value. Rhodamine B in methanolic solutions is known to exhibit radiative excited-state deactivation that follows a single-exponential decay law.[32] Maps of both fluorescence lifetime and

(28) Benninger, R. K. P.; Onfelt, B.; Neil, M. A. A.; Davis, D. M.; French, P. M. W. *Biophys. J.* **2005**, *88*, 609−622.
(29) Denk, W.; Strickler, J. H.; Webb, W. W. *Science* **1990**, *248*, 73−76.
(30) Requejo-Isidro, J.; McGinty, J.; Munro, I.; Elson, D. S.; Galletly, N. P.; Lever, M. J.; Neil, M. A. A.; Stamp, G. W. H.; French, P. M. W.; Kellett, P. A.; Hares, J. D.; Dymoke-Bradshaw, A. K. L. *Opt. Lett.* **2004**, *29*, 2249−2251.
(31) Dowling, K.; Hyde, S. C. W.; Dainty, J. C.; French, P. M. W.; Hares, J. D. *Opt. Commun.* **1997**, *135*, 27−31.
(32) Moog, R. S.; Ediger, M. D.; Boxer, S. G.; Fayer, M. D. *J. Phys. Chem.* **1982**, *86*, 4694−4700.

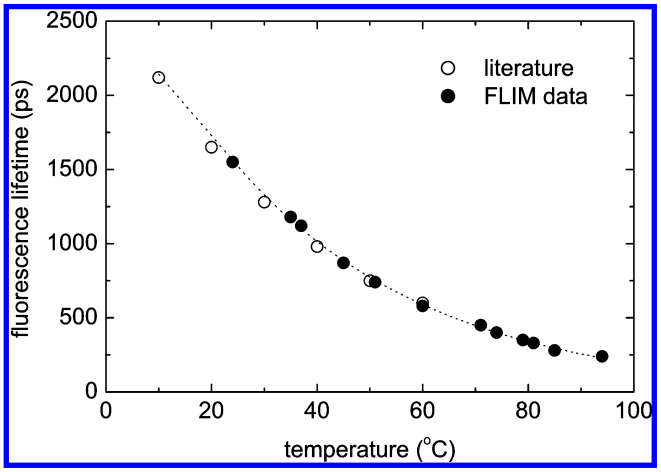


**Figure 2.** Measured fluorescence lifetime for rhodamine B in methanolic solution as a function of temperature (●) and published fluorescence lifetime data as a function of temperature (○). An exponential trend line was fitted to both data sets and used for temperature calibration ($\lambda^{2p}_{ex}$ = 840 nm, $\lambda_{em}$ ~ 580 nm).

fluorescence intensity are combined as a false color scale image in HSV (hue−saturation−value) format, where hue represents fluorescence lifetime, saturation is at a constant maximum, and value represents the integrated fluorescence intensity. Temperature can be deduced from the fluorescence decay time via a calibration curve, which may be generated from prior measurements of the fluorescence lifetime of homogeneous (~2 mL) solutions of rhodamine B as a function of temperature. We note that calibration data from the literature can also be used for this process (for example, data reported in reference 33), since recovered lifetimes are independent of system parameters, unlike time-integrated fluorescence measurements.

## RESULTS & DISCUSSION

**System Calibration.** Fluorescence lifetime values for methanolic solutions of rhodamine B were measured for a range of temperatures, as displayed in Figure 2. The lifetime decreases with temperature, which is thought to be due to an increase in rotation of the diethylamino group that facilitates more efficient nonradiative deactivation of the excited state.[34] A similar temperature dependence of the rhodamine B fluorescence lifetime in methanolic solutions has been reported previously.[33] We observe empirically that the data fits well to an exponential decay with a deviation from the trend line of <2 °C over the whole temperature range of 25−95 °C. We note that for many applications, it would be desirable to determine temperature distributions in aqueous solution. The temperature dependence of the fluorescence lifetime of rhodamine B is almost identical in aqueous and methanolic solvents,[33,34] and hence, the use of aqueous solutions is equally possible. We note that heating induced by the laser beam used

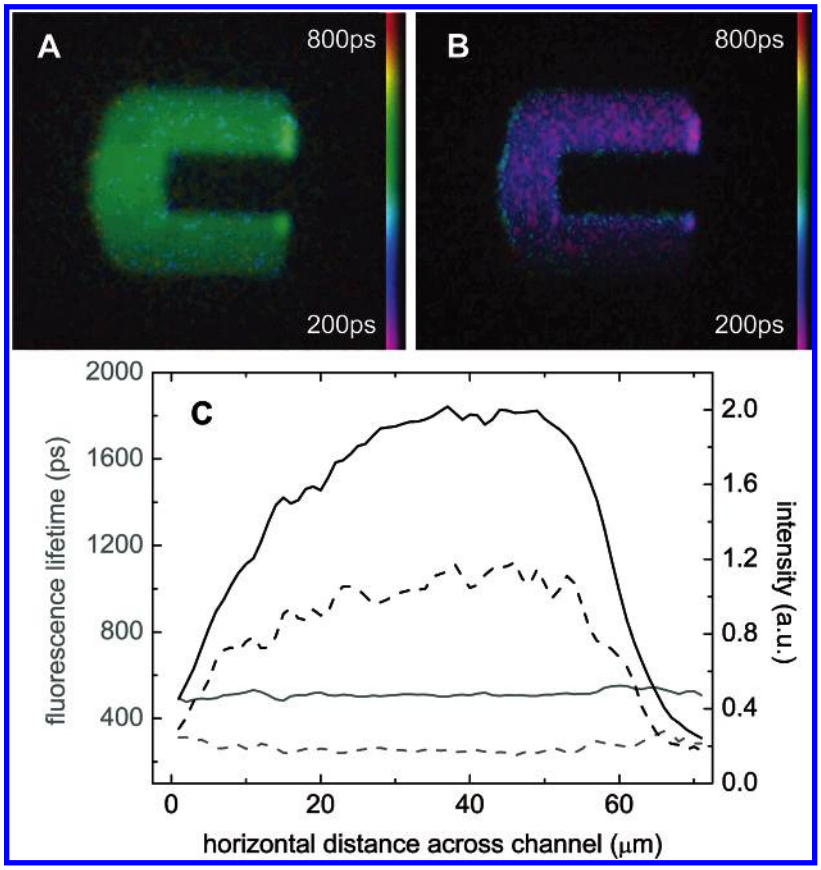


**Figure 3.** Representative fluorescence lifetime data from methanolic solutions of rhodamine B in microchannels. Fluorescence lifetime images taken at the same spatial position for 66 (A) and 93 °C (B) heating. (C) Profile of fluorescence lifetime (light gray lines) and time-integrated intensity (black lines) across the microchannel width. The fluorescence lifetime is approximately constant over the width of the microchannel, with minimal statistical noise. Both the fluorescence intensity and lifetime decrease between 66 (solid line) and 93 °C heating (dashed line) by a factor of ~2. Whereas the fluorescence intensity is a function of excitation/detection efficiency, fluorophore concentration, and temperature, the fluorescence lifetime is solely a measure of temperature; hence, the much flatter profile, which is consistent with a constant fluid temperature across the microchannel.

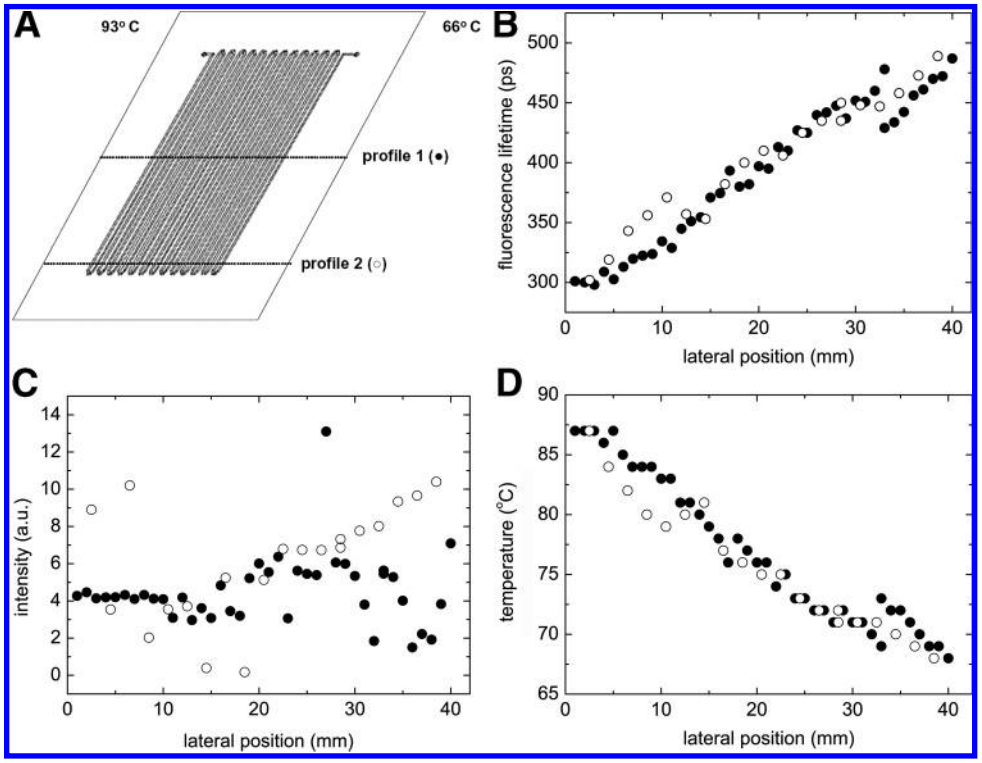


**Figure 4.** (A) Schematic of chip arrangement for temperature measurements. The left-hand side of the device was maintained at 93 °C with the right-hand side being maintained at 66 °C. Data are recorded from two collinear scans along the temperature gradient, denoted profile 1 and profile 2. (B) Variation of fluorescence lifetime data as a function of lateral position across the microfluidic device. (C) Uncalibrated time-integrated intensity data as a function of lateral position across the microfluidic device. (D) Fluidic temperature profiles determined from fluorescence lifetime data.

for the fluorescence lifetime measurements was negligible, which is consistent with previously published findings for bulk solution.[35]

**Imaging Fluidic Temperature in Microchannels.** In initial experiments, a methanolic solution of rhodamine B was pumped through a glass microfluidic device at a volumetric flow rate of 0.1 $\mu$L/min, and time-gated intensity images were acquired. Temperatures in the microchannels were controlled through contact heating at the chip surface. Figure 3 illustrates representative fluorescence lifetime data from regions of the microfluidic channel maintained at 66 °C (Figure 3A) and 93 °C (Figure 3B), as typically used for thermal cycling in on-chip PCR. Acquisition times were tyically 10−30 s per fluorescence lifetime image, which was compatible with the steady-state flow and heating conditions. No photobleaching was observed. Visual inspection of these images clearly shows a different rhodamine B fluorescence lifetime at the two regions. Examination of both lifetime profiles and time-integrated fluorescence intensity profiles across the channel width (Figure 3C) reveals that both the fluorescence lifetime and intensity are reduced by a factor of ~2 at the higher temperature. It should also be noted that, although the fluorescence intensity falls off at the channel edges (due to reduced excitation efficiency and concentration effects), the measured lifetime remains constant across the entire channel width.

To demonstrate the robustness of the approach, fluorescence lifetime images were acquired at different spatial locations across the chip, with the entire device maintained at either 66 or 93 °C. For 66 °C heating, the mean rhodamine B lifetime averaged over all spatial points was 496 ± 15 ps, whereas for 93 °C, heating, the mean lifetime was 277 ± 16 ps. Using the previously calibrated temperature dependence of the rhodamine B fluorescence lifetime in methanolic solution, the apparent temperatures were calculated as 66.5 ± 1 and 90 ± 2 °C, respectively. Errors bars in this case refer to statistical error in mean lifetime due to spatial fluctuations and are consistent with estimated errors in the temperature measurement discussed previously. For the 66 °C region, the observed temperature of the fluid is in good agreement with the corresponding heating block temperature, but for the 93 °C region, the observed temperature is slightly lower. This is in part due to increased heat dissipation from the substrate at higher temperatures. The spatial variation in the measured fluorescence lifetime across the chip corresponds to an equivalent temperature variation of 3 °C standard deviation. This is the case for both 66 and 93 °C heating and lies within the temperature bounds for efficient PCR.

**Imaging Microfluidic Temperature Gradients.** In some microfluidic applications, such as continuous flow PCR,[36] two or more distinct temperature zones are required to allow thermal cycling of reagents. Reagents flow across temperature zones, experiencing the required temperatures for a time period that is determined by the applied flow rate, microchannel dimensions, and heating area. To indicate the potential use of fluorescence lifetime imaging for measuring fluidic temperatures in such systems, we acquired time-integrated fluorescence intensity images and fluorescence lifetime images at different points along a serpentine microchannel (and across the microfluidic device) under an applied temperature gradient. This gradient was created across the length of the chip using the heating cartridges as a parallel heat source and sink. Figure 4A shows a schematic of the measurement points along the temperature gradient, with

Figure 4B showing the corresponding fluorescence lifetime variations. It can be seen that fluorescence lifetime data obtained in each linear scan are consistent and demonstrate an increase in fluorescence lifetime from 300 to ~500 ps. Figure 4C illustrates the equivalent variation in integrated fluorescence intensity. Although some variation is observed, consistent with fluorescence lifetime variation, the varying excitation/detection efficiencies across the microchip render the intensity data unsuitable for temperature determination, without ratioing or prior excitation/detection efficiency calibration. In contrast, temperature variation can be calculated from the fluorescence lifetimes using published calibration data, as shown in Figure 4D. Interestingly, the optimum fluid temperatures of 65−68 °C in the low temperature zone are only obtained within ~5 mm of the corresponding heating block, whereas fluid temperatures in the high-temperature zone are below the 92−95 °C optimum. This will need to be taken into account in future PCR chip designs. For the existing noninsulated heating system, this will, for instance, require a modified channel layout with meandering channel segments only at the edges of the microchip and stronger heating in the high-temperature zone. The observed temperature variation is consistent with theoretical modeling-derived substrate temperatures for similar heating configurations.[37]

**3D-Mapping of Channel Temperature.** In applications such as PCR, the 3D intrachannel temperature distribution, in the presence of flow, is important for defining the reaction efficiency. Experiments were undertaken to demonstrate how fluorescence lifetime imaging could quantitatively map fluidic temperatures in three dimensions with micrometer spatial resolution. Figure 5A illustrates a rendered 3D image of fluorescence lifetime data corresponding to a 100-$\mu$m-long microchannel segment containing a methanolic solution of rhodamine B moving at a volumetric flow rate of 10 $\mu$L/min. In this system, the microchannel is in contact with a heating element placed close to the upper channel surface. As expected, there is a fluorescence lifetime variation across the microchannel corresponding to a 3D temperature variation. Specifically, the fluorescence lifetime can be seen to increase as a function of distance away from the upper channel surface, with a change in fluidic temperature of ~5 °C. This temperature variation is quantified in Figure 5B, for which vertical fluorescence lifetime line profiles have been sampled and converted into temperature for volumetric flow rates of 0.1 and 10 $\mu$L/min. The corresponding horizontal line profiles are shown in Figure 5C. The horizontal profiles at half channel depth reveal a flat temperature profile of 68.5 ± 0.5 and 67.5 ± 0.5 °C under 0.1 and 10 $\mu$L/min flow rates, respectively, with an ~2 °C increase at the extreme edges. The use of two-photon excitation and the associated optical sectioning phenomena provide for a spatial resolution of ~1 $\mu$m in the lateral direction and 10 $\mu$m in the axial dimension. We note that due to the ~1-mm-thick microfluidic substrate, a long working distance, low-NA objective was employed here, limiting the axial resolution and signal intensity. The use of high-NA objectives, as previously demonstrated,[23] would result in significantly improved performance, with submicrometer axial resolution and low-noise data.

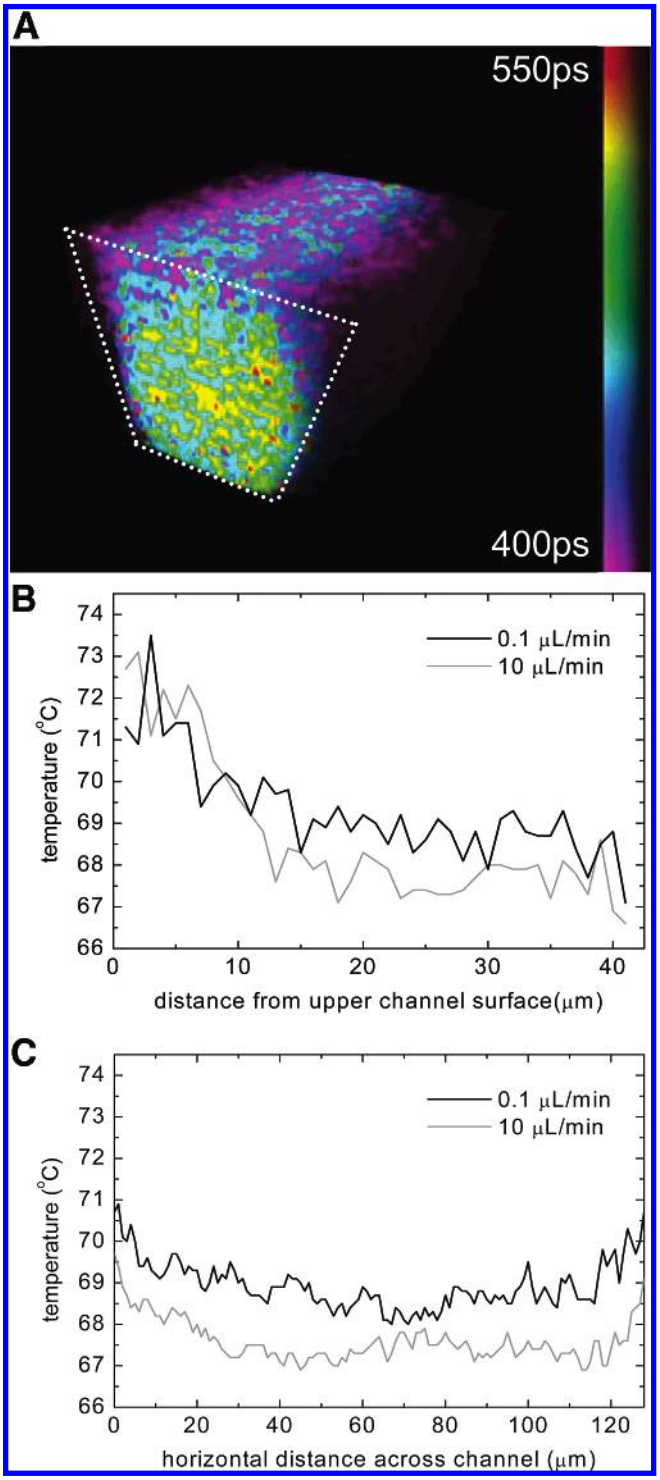


**Figure 5.** 3D temperature mapping of fluidic temperatures. (A) False-color-rendered 3D image of fluorescence lifetime variations of a methanolic solution of rhodamine B within a 130 × 40 × 100-$\mu$m microchannel segment and at a flow rate of 10 $\mu$L/min. Channel boundaries are indicated by white dotted lines. The upper surface of the microchannel is held at 73 °C. (B) Variation of temperature as a function of distance away from the upper microchannel surface at volumetric flow rates of 0.1 and 10 $\mu$L/min. (C) Variation of temperature as a function of distance across the microchannel at half channel depth at volumetric flow rates of 0.1 and 10 $\mu$L/min.


(33) Kitamura, N.; Hosoda, Y.; Ueno, K.; Iwata, S. *Anal. Sci.* **2004**, *20*, 783−786.
(34) Kitamura, N.; Hosoda, Y.; Iwasaki, C.; Ueno, K.; Kim, H. B. *Langmuir* **2003**, *19*, 8484−8489.
(35) Dittrich, P. S.; Schwille, P. *App. Phys. B: Lasers Opt.* **2001**, *73*, 829−837.
(36) Kopp, M. U.; de Mello, A. J.; Manz, A. *Science* **1998**, *280*, 1046−1048.
(37) Hao, Q. *J. Micromech. Microeng.* **2004**, *14*, 914−926.

## CONCLUSIONS

We have demonstrated for the first time that fluorescence lifetime imaging can be applied to the accurate measurement of intrachannel temperature variations in microfluidic systems. Determining the molecular fluorescence lifetime is essentially a ratiometric measurement and so avoids many of the problems associated with intensity artifacts that hinder the application of conventional (steady-state) optical imaging techniques. Accordingly, this technique should be useful for imaging temperature distributions in turbid samples through nonuniform structures, such as curved capillaries or PDMS microchips.[23] A notable feature of the implementation reported here is the use of two-photon excitation, which provides inherent optical sectioning and, thus, enhances quantitation of system parameters, such as temperature, as well as permits three-dimensional temperature mapping with micrometer spatial resolution. For these initial studies, we have demonstrated that FLIM of rhodamine B in microfluidic channels can provide spatially resolved maps of fluidic temperature distributions with a precision of ±1 °C. Further improvements in sensitivity are possible, for example, using a dye that exhibits a larger change in quantum yield as a function of temperature. Higher NA excitation and detection would also allow both lateral and axial resolution to be significantly enhanced, to a submicrometer scale. This would also improve signal through enhanced two-photon excitation efficiency and allow the potential for video rate FLIM, previously applied in on-chip viscosity measurements.[23] We also note that, although the equipment discussed here may be considered complex by a nonspecialist, there are simpler and cheaper wide-field optically sectioned fluorescence imaging techniques that may be used, such as structured illumination,[38] as well as miniaturized or on-chip 3D fluorescence techniques.[39,40] Additionally, frequency domain FLIM can be implemented with LED excitation sources and low-cost mobile phone circuitry.[41] This bodes well for the wider availability of this powerful approach for on-chip measurements of microfluidic processes.


(38) Neil, M. A. A.; Squire, A.; Juškaitis, R.; Bastiaens, P. I. H.; Wilson, T. *J. Microsc.* **2000**, *197*, 1−4.

(39) Jung, J. C.; Schnitzer, M. J. *Opt. Lett.* **2003**, *28*, 902−904.

(40) Paul, U. P.; Li, L.; Lee, M. L.; Farnsworth, P. B. *Anal. Chem.* **2005**, *77*, 3690−3693.

(41) Booth, M. J.; Wilson, T. *J. Microsc. (Oxford)* **2004**, *214*, 36−42.



## ACKNOWLEDGMENT

The authors acknowledge financial support from a Department of Trade and Industry (DTI) Beacon award, the European Community (Framework VI Integrated Project *Integrated technologies for in vivo molecular imaging* contract number LSHG-CT-2003-503259), Engineering and Physical Sciences Research Council (EPSRC), and Molecular Vision Ltd. R.K.P.B. acknowledges the award of a CASE studentship from EPSRC and Kentech Instruments Ltd. Y.C. thanks Smiths Detection for the provision of a research studentship.

Received for review November 8, 2005. Accepted January 9, 2006.

AC051990F